Hindawi Publishing Corporation
Advances in Optical Technologies
Volume 2012, Article ID 247070, 10 pages
doi:10.1155/2012/247070

Review Article

Dynamics of 1.55 μm Wavelength Single-Mode Vertical-Cavity Surface-Emitting Laser Output under External Optical Injection

Kyong Hon Kim, Seoung Hun Lee, and Vijay Manohar Deshmukh

Department of Physics, Inha University, Incheon 402-751, Republic of Korea

Correspondence should be addressed to Kyong Hon Kim, kyongh@inha.ac.kr

Received 21 May 2012; Accepted 22 September 2012

Academic Editor: Zoran Ikonic

We review the temporal dynamics of the laser output spectrum and polarization state of 1.55 μm wavelength single-mode (SM) vertical-cavity surface-emitting lasers (VCSELs) induced by external optical beam injection. Injection of an external continuous-wave laser beam to a gain-switched SM VCSEL near the resonance wavelength corresponding to its main polarization-mode output was critical for improvement of its laser pulse generation characteristics, such as pulse timing-jitter reduction, linewidth narrowing, pulse amplitude enhancement, and pulse width shortening. Pulse injection of pulse width shorter than the cavity photon lifetime into the SM VCSEL in the orthogonal polarization direction with respect to its main polarization mode caused temporal delay of the polarization recovery after polarization switching (PS), and its delay was found to be the minimum at an optimized bias current. Polarization-mode bistability was observed even in the laser output of an SM VCSEL of a standard circularly cylindrical shape and used for all-optical flip-flop operations with set and reset injection pulses of very low pulse energy of order of the 3.5~4.5 fJ.

1. Introduction

Dynamical laser output of the vertical-cavity surface-emitting lasers (VCSELs) under injection of an external laser beam has been investigated widely for potential application to pulse timing-jitter reduction, polarization switching, all-optical flip-flop operation, and long-distance fiber transmissions [1–15]. VCSELs are known to be low power-consuming optical signal sources compared to the existing edge-emitting laser diodes (LDs) and to be potentially useful all-optical logic gate devices in a two-dimensional array. Beside the conventional signal source application of the stand-alone VCSELs for relatively short-distance optical communications or interconnects, the injection locking of an external optical beam to the VCSELs allows new application areas of the VCSELs possible and improves fiber transmission properties of the VCSELs' output. Weak continuous-wave (CW) laser beam injection to a gain-switched VCSEL lowered its pulse timing jitter [2, 3]. Laser pulse beam injection of an orthogonal or circular polarization into a VCSEL caused a high-speed polarization switching (PS) [4–7] or spin-induced polarization oscillation [8, 9]. The PS and induced bistability mechanism of the VCSEL output under a laser beam injection of orthogonal polarization to the VCSEL's main polarization mode were used for demonstration of all-optical flip-flop operation and optical buffer memory application [10–13]. An external laser beam injection to high-speed direct-modulated VCSELs reduced the frequency chirp, enhanced the small-signal modulation bandwidth, and thus helped extension of the transmission distance of the VCSEL signals over long fiber spans [14–16].

In this paper, we will first review what optimum external beam injection condition required for the gain-switched VCSELs to have the minimized timing jitter state. Then, we discuss how the polarization-switching dynamics vary with external optical beam injection conditions. Finally, we introduce how the PS dynamics can be used for high-speed all-optical flip-flop application.

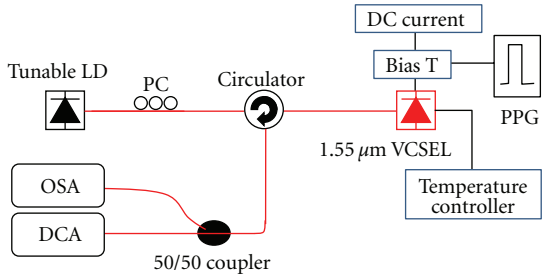

Figure 1: Experimental setup used for the timing-jitter reduction of the gain-switched VCSEL pulses with a laser beam injection; PPG: pulse pattern generator; PC: polarization controller, OSA: optical spectrum analyzer; DCA: digital communication analyzer.

2. Timing-Jitter Reduction of Gain-Switched Single-Mode VCSELs

Gain-switched or mode-locked optical pulses of low timing jitter are very useful for high-speed optical time-division multiplexed communications and all-optical signal processing. It has been demonstrated previously that the timing jitter of gain-switched semiconductor lasers, such as Fabry-Perot (FP) LDs and distributed feedback (DFB) LDs, could be reduced by an external laser beam injection [17, 18]. However, it was observed that a trade-off relationship existed between the jitter reduction and pulse width shortening of the gain-switched LDs.

Recently, timing-jitter reduction as well as pulse width shortening, pulse amplitude enhancement, spectral linewidth narrowing, and pulse amplitude increase of gain-switched pulses from a 1.55 μm wavelength single-mode VCSEL was observed experimentally with an optimized injection laser beam wavelength [3]. Figure 1 shows the experimental setup used for timing-jitter reduction of the gain-switched VCSEL pulses with a tunable laser beam injection. The VCSEL was a commercially available single-longitudinal- and transverse-mode (SM) VCSEL based on monolithically grown InAlGaAs-InGaAs quantum well layers emitting a laser beam at 1.55 μm wavelength. It was packaged into a transistor-outlined-can (TO-CAN) with a single-mode fiber (SMF) pigtail and with a thermoelectric cooler (TEC) inside. This TO-CAN type-packaged VCSEL had a threshold current of about 2.1 mA at 21.4°C. The VCSEL was gain switched by rectangular electric pulses of 400 ps pulse width and 280 mV amplitude at 1.25 GHz repetition rate with a DC bias current of 3 mA, while its temperature was kept at 21.4°C with the TEC control.

Figure 2(a) shows measured optical spectra of the free-running continuous-wave (CW) and gain-switched VCSEL's outputs with an optical spectrum analyzer (OSA). The free-running CW spectrum illustrates the linearly polarized main mode at 1,553.86 nm with a 3 dB linewidth below the OSA resolution limit of 0.06 nm, while the side mode of orthogonal polarization appears at a shifted wavelength of 0.35 nm from the main mode with its intensity suppressed relatively below 32 dB from the main peak. The gain switching caused spectral broadening of the two polarization-mode outputs

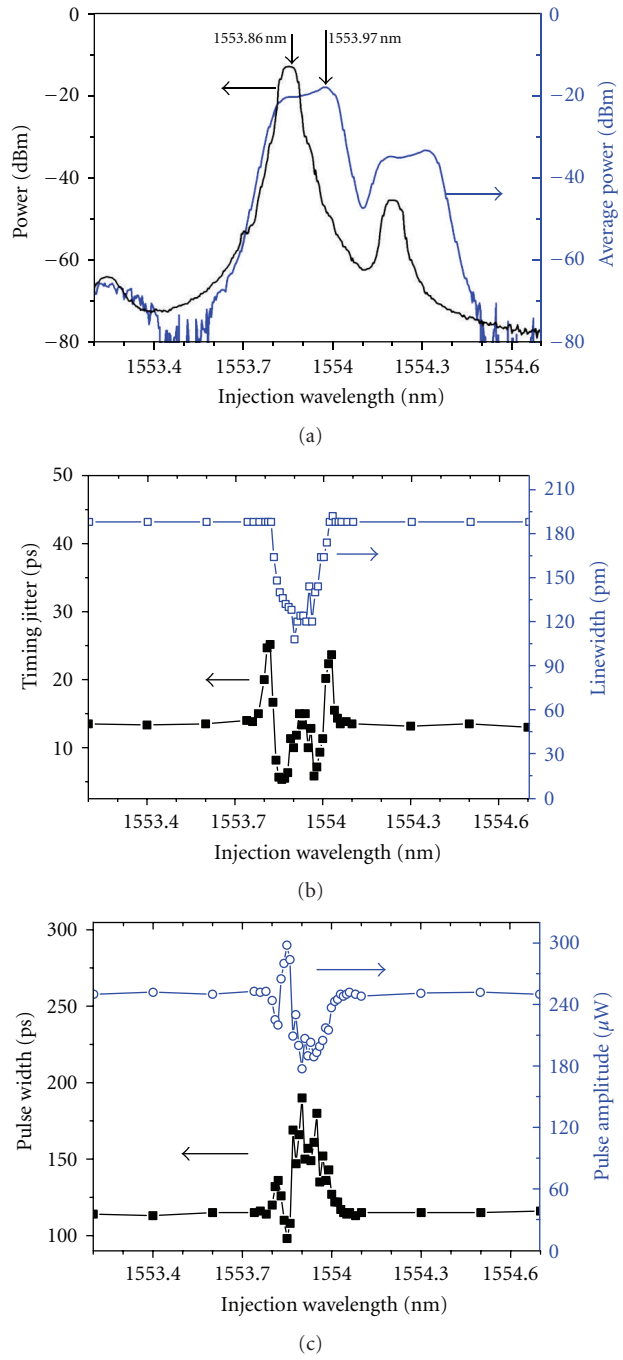

Figure 2: (a) Measured optical spectra of the VCSEL in a free-running continuous-wave (black line with the Y-axis scale on the left-hand side) and gain-switched operations (blue line with the Y-axis scale on the right-hand side); measured (b) timing jitter and linewidth; (c) pulse width and pulse amplitude of the gain-switched VCSEL pulses under an external laser beam injection.

probably due to the gain-modulated spectral chirping inside the VCSEL. Then, a CW optical beam from a tunable laser source was coupled into the VCSEL via an optical circulator and polarization controller (PC) in the same polarization direction as that of the main mode. Figures 2(b) and 2(c) show the measured root-mean-square (rms) timing jitter,

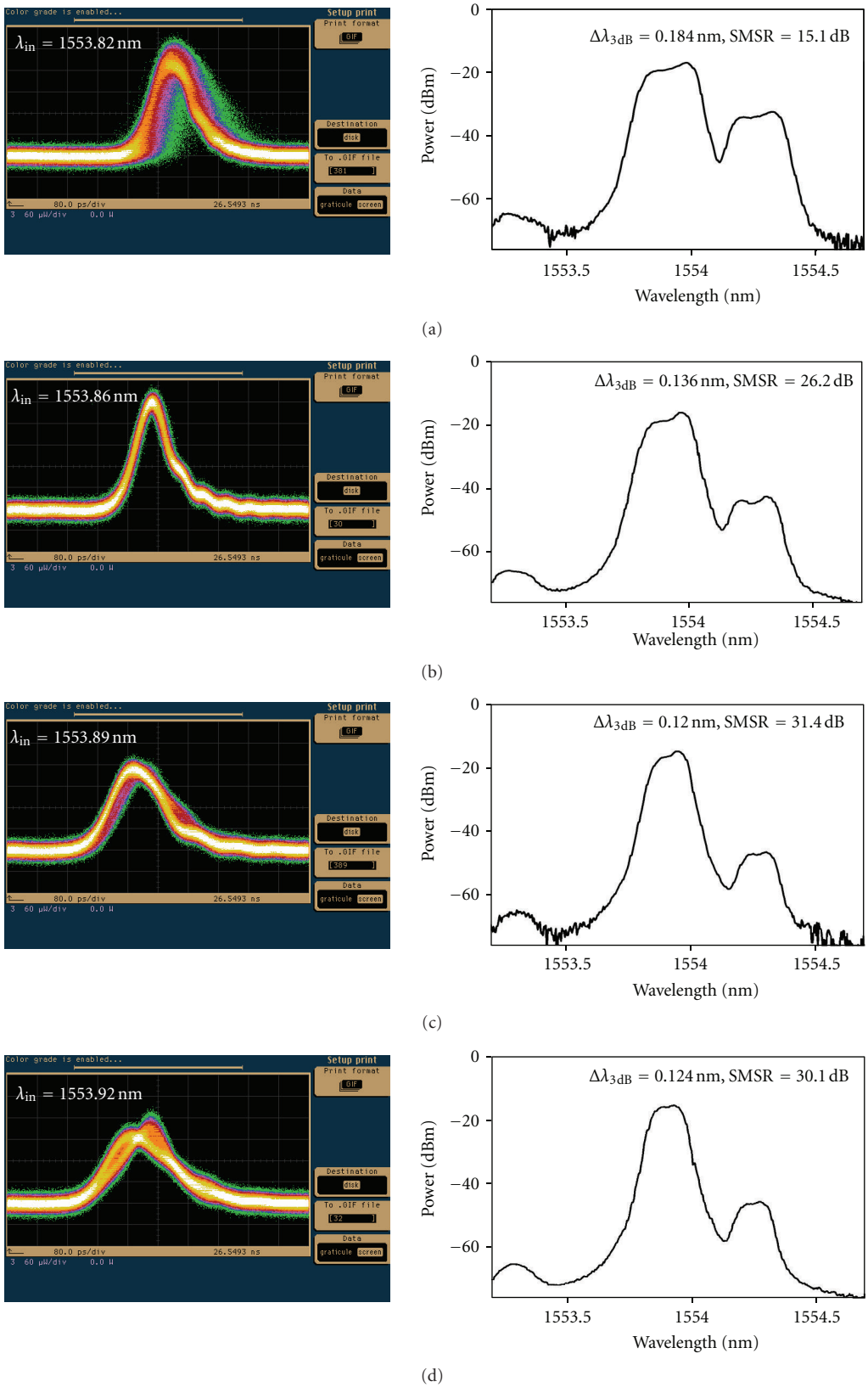

Figure 3: The measured pulse shapes and optical spectra of the gain-switched pulses with external beam injection of various detuned wavelengths.

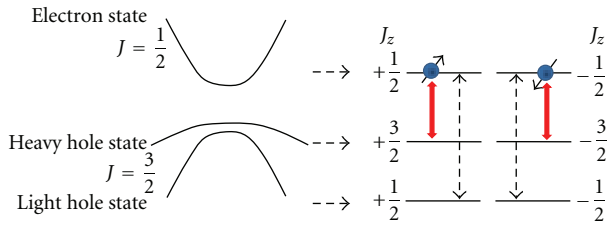

FIGURE 4: The band structure of semiconductor quantum wells and allowed transitions [19].

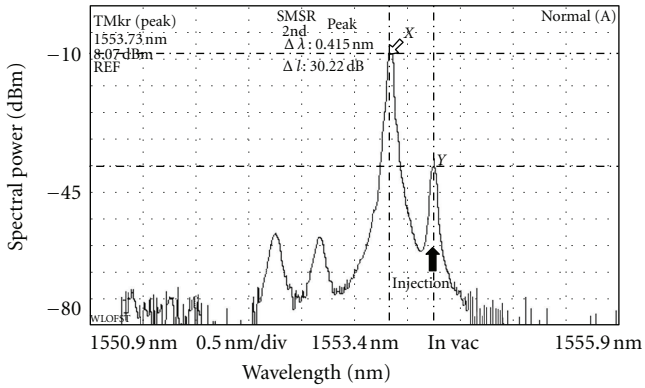

FIGURE 5: Observed output spectrum of a single-mode 1.5 μm wavelength VCSEL.

spectral linewidth, and time-averaged pulse width and pulse amplitude of the gain-switched VCSEL output under the external tunable laser beam injection while the injection, beam wavelength was tuned from 1,553.2 nm to 1,554.7 nm. The laser power and 3 dB linewidth of the injection beam were −23 dBm and below the OSA resolution limit of 0.06 nm, respectively. Fine-tuning of the injection laser beam wavelength allowed an optimized condition of the pulse width shortening, pulse amplitude enhancement, spectral linewidth narrowing, and pulse amplitude increasing near the free-running main-mode peak wavelength unlikely to the previously reported results of trade-off relationship between the jitter reduction and pulse width shortening.

Figure 3 shows the measured oscilloscope traces and optical spectra of the gain-switched VCSEL pulses under laser beam injections at various detuned wavelengths. The optimum injection wavelength for the minimum jitter and narrow linewidth matches closely with the main-mode wavelength of 1,553.86 nm which corresponds to the resonant transition between the electron spin sublevels ($J_z = \pm 1/2$) of the conduction band and the heavy hole sublevels ($J_z = \pm 3/2$) of the valence band as illustrated in Figure 4. This low time-jittered gain-switched VCSEL pulse sources with an optimized injection scheme will be useful for power-efficient high-speed optical TDM communications, high-speed all-optical sampling, high-speed all-optical signal processing, and low-error quantum key distribution applications.

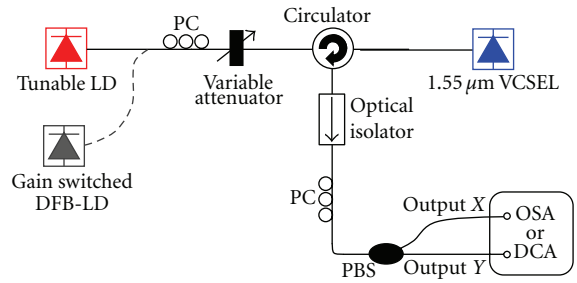

FIGURE 6: Experimental setup used for study of PS dynamics of a single-mode 1.5 μm wavelength VCSEL. PC: polarization controller, PBS: polarization beam splitter.

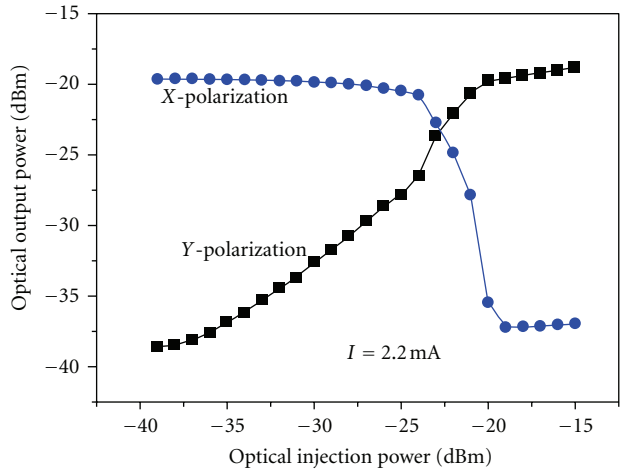

(a)

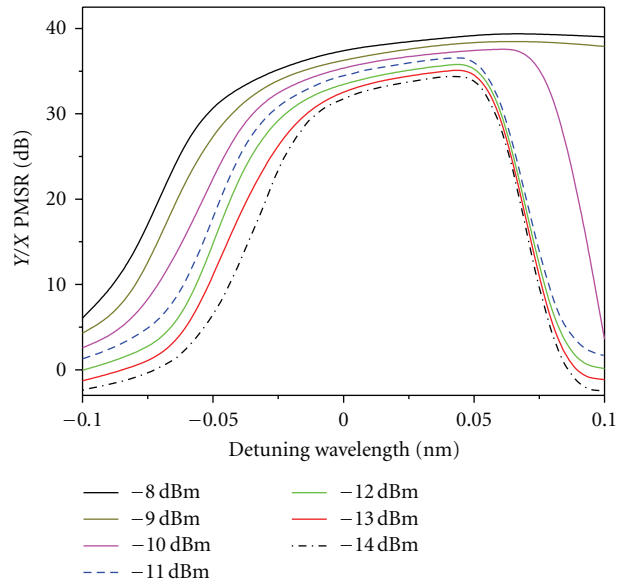

(b)

FIGURE 7: Observed (a) PS dynamics of the single-mode 1.5 μm wavelength VCSEL as a function of the optical injection powers with a driving current slightly above threshold and (b) PMSR as a function of the injection wavelength detuning for various injection powers.

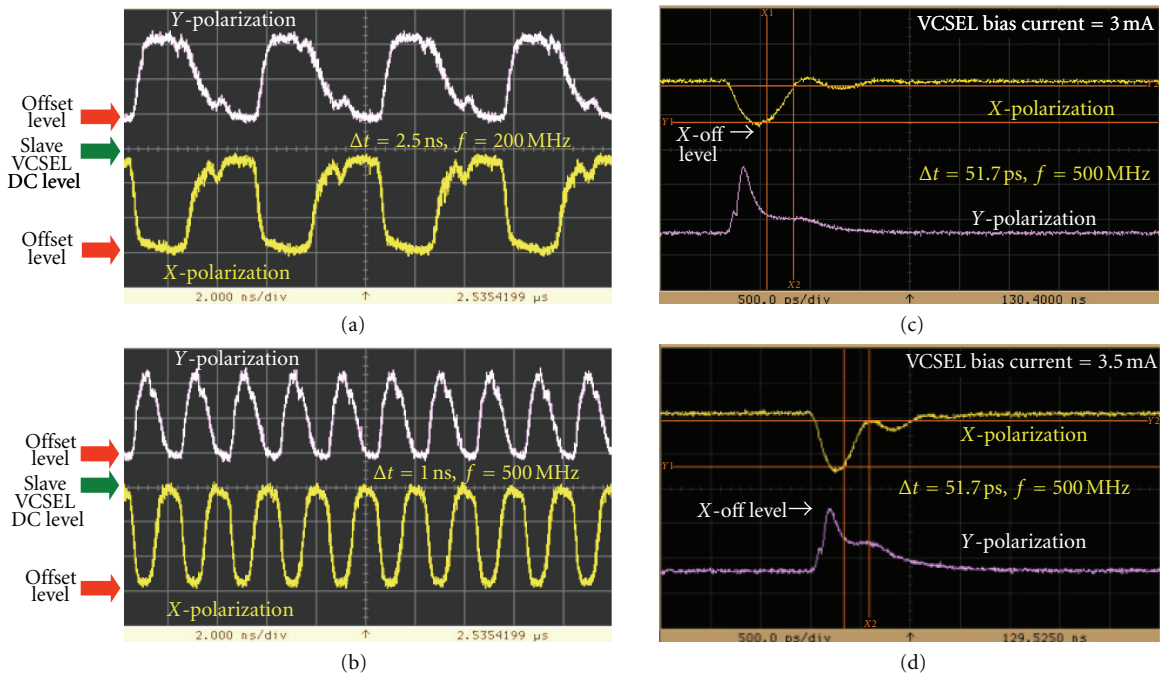

FIGURE 8: Temporal response of the PS dynamics of an SM 1.5 μm wavelength VCSEL with an operating DC bias current of I_b under external beam injection of pulse width (Δt) and repetition rate (f). (a) $\Delta t = 2.5$ ns and $f = 200$ MHz, $I_b = 3.0$ mA, (b) $\Delta t = 1.0$ ns and $f = 500$ MHz, $I_b = 3.0$ mA, (c) $\Delta t = 51.7$ ps and $f = 500$ MHz, $I_b = 3.0$ mA, and (d) $\Delta t = 51.7$ ps and $f = 500$ MHz, $I_b = 3.5$ mA.

3. Polarization Switching Dynamics

Polarization switching (PS) dynamics of the VCSELs with an external optical beam injection have been the focus of significant research effort because of the potential applications to optical flip-flop operation, all-optical signal processing, optical communications, and photonic switching [4–13, 20]. Early stage of the PS research in VCSELs mainly focused on multimode (MM) VCSELs at 850 nm wavelength, which was then followed by the PS dynamics study in 980 nm and 1.3 μm wavelength VCSELs, a special square-shaped SM 1.5 μm wavelength VCSEL, or an MM 1.5 μm VCSEL. The first experimental demonstration of the optical injection-induced PS property of conventional circularly cylindrical-shaped single-transverse-mode 1.5 μm wavelength VCSELs based on InAlGaAs quantum wells on InP wafers was demonstrated in [4]. Even though the circularly cylindrical-shaped SM VCSEL is supposed to have a circular symmetry, it possesses a dominant polarization-mode output at a driving current above threshold as shown in Figure 5. Depending on VCSEL chips, there is a side mode corresponding to the orthogonal polarization of the dominant main mode in a separated wavelength of subnanometer. The side-mode suppression ratio (SMSR) is usually larger than 30 dB.

Figure 6 shows the experimental setup of all-fiber-type configuration used for measurement of polarization switching of an SM 1.5 μm wavelength VCSEL with a CW tunable laser beam injection. Experimentally observed PS dynamics of the VCSEL with a driving current of 2.2 mA slightly above threshold ($I_{\text{th}} = 1.6$ mA) as a function of the optical injection power are shown in Figure 7(a), and the measured polarization mode suppression ratio (PMSR) between Y- and X-polarizations as a function of the injection wavelength detuning for various injection powers is also shown in Figure 7(b). The tunable LD beam was injected at the polarization direction orthogonal to that of the main-polarization mode of the free-running VCSEL output.

When a gain-switched distributed feedback (DBF) LD was used for optical pulse injection in Figure 6 instead of the CW tunable LD, delayed response of polarization switching and polarization recovery was also observed [4, 7]. For long injection pulses at relatively low repetition rate, no significant time delay of the polarization switching and recovery was observed as shown in Figures 8(a) and 8(b) [21]. However, as the injection pulse width becomes shorter than or close to 50 ps, a significant delay in the polarization switching and recovery was observed as shown in Figures 8(c) and 8(d).

The temporal behavior of polarization dynamics was numerically analyzed using the spin-flip model (SFM) [7, 19]. The SFM describes the electrical fields of the X- and Y-polarizations, E_x and E_y, related to the excited population N and the population difference n between spin-up and spin-down radiation channels as

$$\frac{dE_x}{dt} = k(1 + j\alpha)\left(NE_x - E_x + jnE_y\right) - \left(\gamma_a + j\gamma_p + j\Delta\omega\right)E_x + \sqrt{\beta_{\text{sp}}}\xi_x,$$

$$\frac{dE_y}{dt} = k(1 + j\alpha)\left(NE_y - E_y - jnE_x\right) + \left(\gamma_a + j\gamma_p - j\Delta\omega\right)E_y + \sqrt{\beta_{\text{sp}}}\xi_y + k_{\text{inj}}E_{\text{inj}},$$

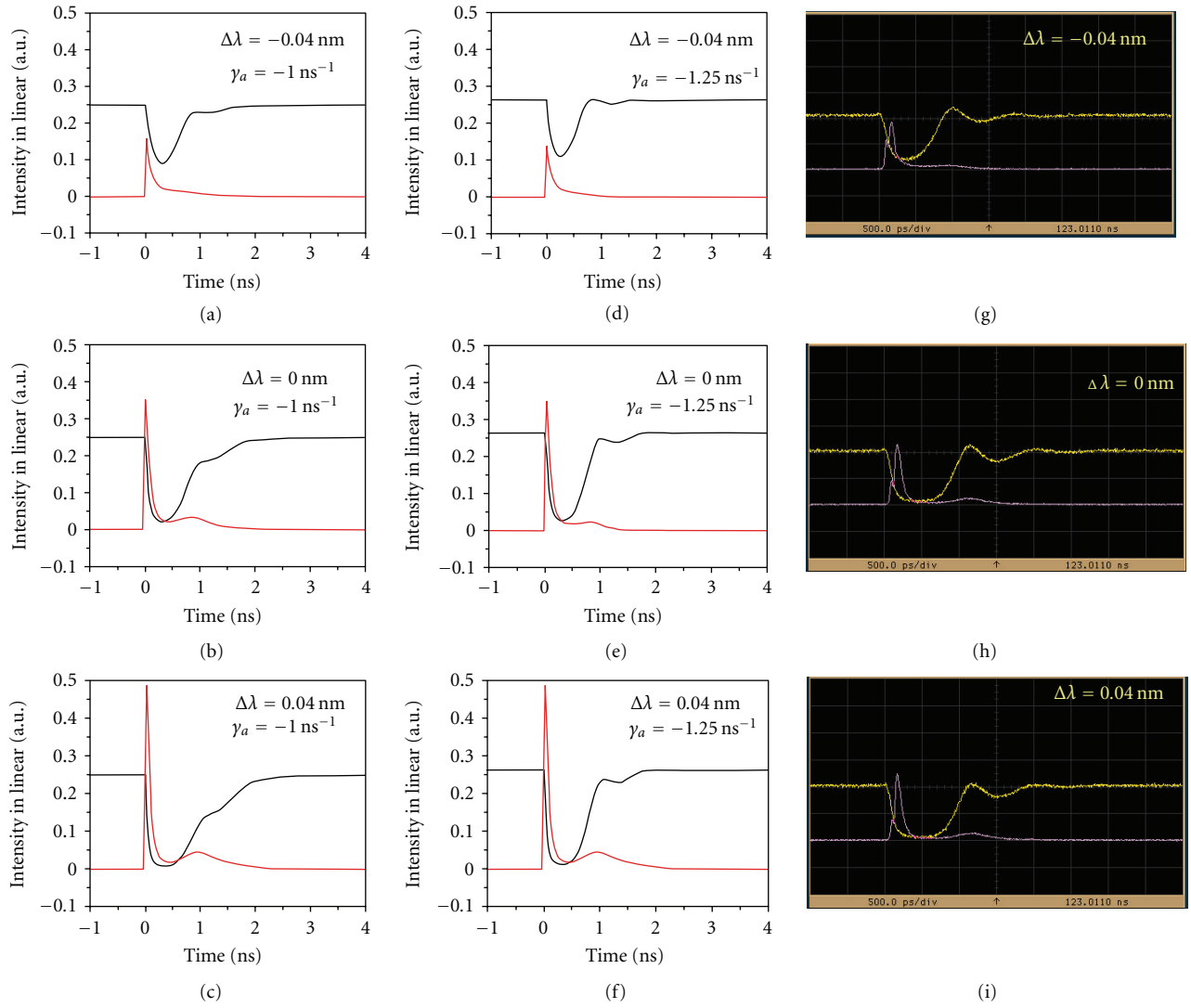

FIGURE 9: Experimentally observed oscilloscope traces compared to numerically calculated plots of the polarization dynamics of an SM VCSEL under injection of short optical pulses of 51.7 ps pulse width for various detuned wavelengths and two linear dichroism parameter values of $-1.0\,\mathrm{ns}^{-1}$ and $-1.25\,\mathrm{ns}^{-1}$.

$$\frac{dN}{dt} = -\gamma_e N(1+P) + \gamma_e \mu - j\gamma_e n\left(E_y E_x^* - E_x E_y^*\right),$$
$$\frac{dn}{dt} = -\gamma_s n - \gamma_e nP - j\gamma_e n\left(E_y E_x^* - E_x E_y^*\right). \tag{1}$$

In the above equations, k is the decay rate of the electric field in the VCSEL cavity ($\approx 25\,\mathrm{ns}^{-1}$), α is the linewidth enhancement factor (=3), β_{sp} is the strength of the spontaneous emission ($=10^{-5}$), and μ is the normalized injection current ($\mu = 1$ for threshold). $P = |E_x|^2 + |E_y|^2$ is the normalized output power; ξ_x and ξ_y are independant Gaussian white noise source with a zero mean and a unit variance in the X- and Y-polarization directions, respectively. E_{inj} represents the electric field amplitude of the injection beam with an assumption of a Gaussian-shaped time-dependant pulse, and $\Delta\omega$ is the frequency detuning between the injection laser wavelength and the suppressed polarization-mode wavelength of the VCSEL. k_{inj} is the coupling coefficient of the injection beam into the VCSEL, γ_a is the linear dichroism, γ_p is the linear birefringence, γ_e is the decay rate of the total population inversion N, and γ_s is the spin-flip rate ($=50\,\mathrm{ns}^{-1}$). From the measured two polarization-mode wavelengths in the spectrum shown in Figure 5, the linear birefringence γ_p is taken as a half of the frequency difference value between them, which is $-26.09\,\mathrm{ns}^{-1}$ [22]. Since the dominant main polarization-mode wavelength is shorter than the other polarization-mode wavelength, the linear dichroism γ_a was taken as a negative value of $-1.25\,\mathrm{ns}^{-1}$ from the best numerical simulation fit condition to the measured data. Figure 9 shows comparative plots of the measured oscilloscope traces and numerically simulated results of the temporal polarization-switching dynamics of an SM VCSEL under injection of

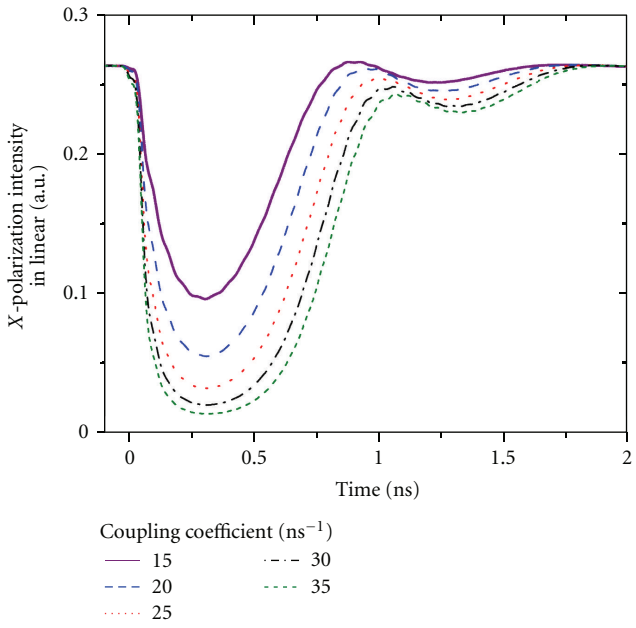

FIGURE 10: Temporal variation of the X-polarized intensity for various values of k_{inj} parameters in ns^{-1} at $k = 25\,\text{ns}^{-1}$.

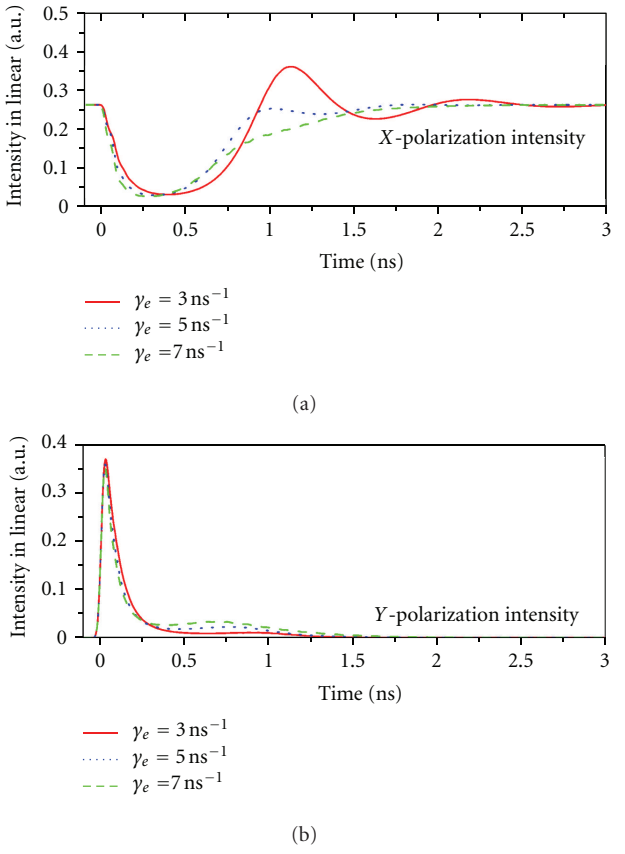

FIGURE 11: Temporal variation of the X- and Y-polarized beam intensities for various values of γ_e parameters in ns^{-1} at $\gamma_a = -1.25\,\text{ns}^{-1}$.

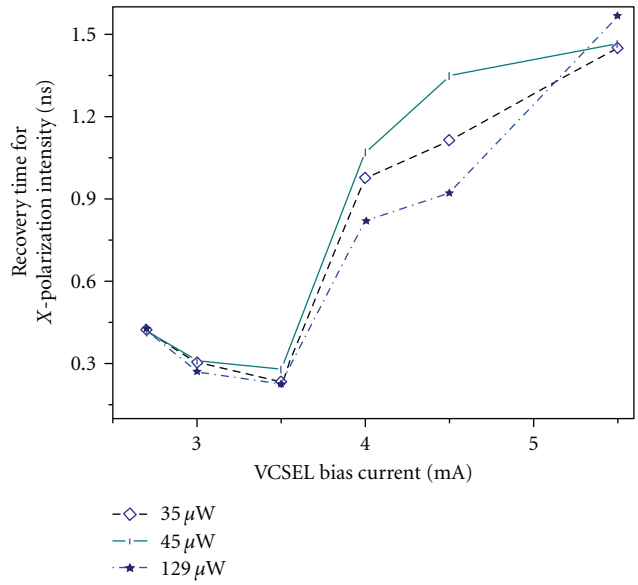

FIGURE 12: Experimentally measured original polarization recovery time as a function of the VCSEL bias current for various peak pulse power of the injection beam.

short optical pulses of 51.7 ps pulse width and 129 μW peak pulse power for three detuned wavelengths and for two linear dichroism parameter values of $\gamma_a = -1.0\,\text{ns}^{-1}$ and $-1.25\,\text{ns}^{-1}$. The simulated results with $\gamma_a = -1.25\,\text{ns}^{-1}$ are better fit to the experimental results.

Numerical simulation of the X-polarization recovery dynamics after injection of a Y-polarization pulse of 50 ps width shows that the optimum value of the coupling coefficient k_{inj} is found to be equal to the field decay rate k (=25 ns^{-1}) as illustrated in Figure 10. In addition, the decay rate of the total excited population γ_e is affected by the linear dichroism parameter γ_a because γ_a is related to the power difference between the X- and Y-polarization-mode outputs. Easy polarization switching takes place for a large γ_e when γ_a is small, while a large decay rate γ_e (i.e., a short decay time) is needed for a large γ_a value to ensure the polarization switching and a short polarization recovery time. Figure 11 shows that the simulated temporal response of the polarization recovery is best fit to the measured one when $\gamma_e = 5\,\text{ns}^{-1}$ for $\gamma_a = -1.25\,\text{ns}^{-1}$.

The delayed polarization recovery after polarization switching on the optical pulse injection could be minimized with an optimum VCSEL bias current. Figure 12 shows the polarization recovery times after the PS due to the external pulse beam injection as a function of the VCSEL bias current for various peak pulse powers of the orthogonal polarization-mode. The results indicates that the optimum VCSEL bias current for the shortest polarization recovery time is 3.5 mA, which is about 1.5 time of threshold current, and is independent of the peak pulse power of the injection beam in the range up to 200 μW. Even at this optimum bias condition, the recovery delay amounts longer than 200 ps. This may be explained with a relatively long photon build-up time in the VCSEL cavity, which is known to be

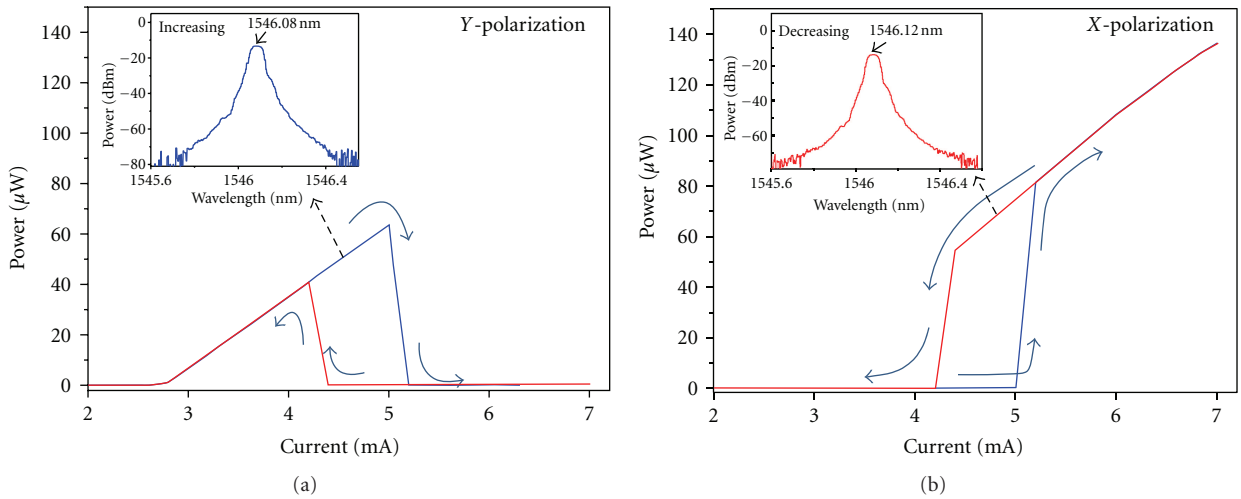

Figure 13: Experimentally measured optical laser output bistability of an SM VCSEL of standard circularly cylindrical shape during increasing and decreasing its bias current.

longer than the photon lifetime [23]. From the consideration of reflectivities of the bottom and top distributed Bragg reflectors (DBRs) of 0.999 and 0.9983 and approximated cavity length of about 10 μm, the estimated photon build-up time based on the photon lifetime calculation inside the VCSEL cavity structure is expected to be longer than 90 ps which is also longer than the pulse width of the injection beam.

The delayed rise time and some relaxation oscillation of the polarization-mode recovery processes after the polarization switching with the optical pulse injection were also observed in [24]. The detailed response may vary from chip to chip even though all the chips are taken from the same wafer. Furthermore, it is reported a fast spin-induced polarization oscillation in VCSELs with injection of a circularly polarized beam, whose process can also be described with the spin-flip model and can be applied potentially for high-speed polarization modulation [8, 9].

4. All-Optical Flip-Flop

All-optical logic gate operation based on laser output bistability properties has been investigated by a few research groups with multi-mode, square-shaped, or standard single-mode-type VCSELs [10–13, 24]. The multi-mode and square-shaped VCSELs require relatively high driving currents compared to the SM VCSELs. The standard SM-type VCSELs of an ideal structure of circularly cylindrical-shape are expected to have no bistability because there is no preferred dominant polarization-mode lasing. However, in practical VCSEL chips fabricated, they are more likely to have a small-gain anisotropy existing in their laser cavity. Thus, this causes some optical bistability in their laser output depending on chip-to-chip basis even though they all are taken from a same wafer [12]. The standard SM-type VCSELs with optical bistability laser outputs can be used for the all-optical flip-flop operation.

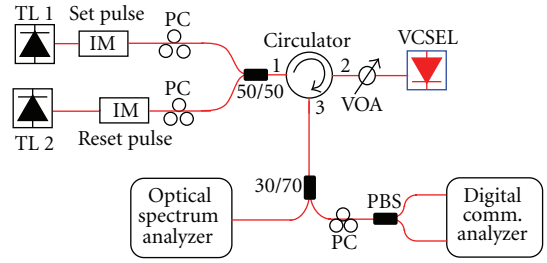

Figure 14: Experimental setup used for the all-optical flip-flop operation on an SM VCSEL of standard circularly cylindrical shape with output bistability. TL: tunable laser; IM: internsity modulator; VOA: variable optical attenuator.

Figure 13 shows the measured optical laser output bistability of a selected InAlGaAs/InP SM VCSEL of standard circularly cylindrical-shape during increasing and decreasing its bias current. During the fine adjustment of the driving bias current to the VCSEL near 4.2 to 5.2 mA, the bistable laser output condition between two polarization modes was observed. Since the laser wavelength of each polarization-mode was separated a little bit from the other, the laser output could be switched between two wavelengths (=1,546.08 nm and 1,546.12 nm) corresponding to two orthogonal polarization modes at the bistability region.

The standard SM VCSEL with the optical bistability property was used for the flip-flop operation by using the experimental setup shown in Figure 14. Two tunable lasers with external modulators were used as set and reset pulse generators, both in orthogonal polarization states to each other and each wavelength corresponding to one of the two polarization modes of the VCSEL at the bistable region, and their modulated beams were injected into the VCSEL through an optical circulator after combined with a 3-dB fiber coupler. The two polarization states of the VCSEL output were separated with a polarization beam splitter

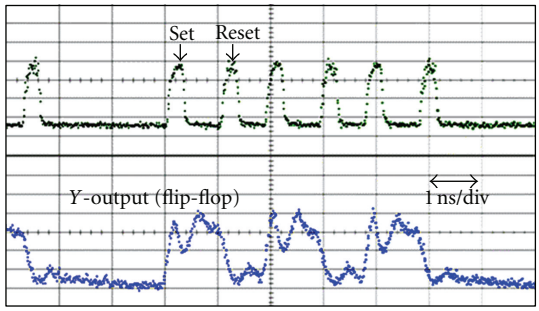

Figure 15: Measured oscilloscope traces of the all-optical flip-flop operated X- and Y-polarization mode outputs of a SM VCSEL with 1 GHz switching frequency of the set and reset pulses.

(PBS), and their temporal dynamics were measured with a digital communication analyzer (DCA).

The flip-flop operation of the VCSEL was performed with set and reset signals, each of which was obtained from the modulated tunable laser pulses of 280 ps pulse width and 112 ps rise time. Figure 15 shows the measured oscilloscope traces of the set and reset pulse trains and of the flip-flop-operated Y-polarization modes of the VCSEL at 1 GHz speed. The switch-on rise and switch-off fall times of the flip-flop-operated signals were 166.9 ps and 215.5 ps, respectively. The pulse energies of the set and reset pulses injected into the VCSEL for the flip-flop operation were only 4.5 fJ and 3.5 fJ, respectively. Further improvement of the flip-flop operation speed can be obtained with a high-speed shorter set and reset pulses.

5. Conclusions

Influence of an external laser beam injection to the SM VCSELs on their laser output characteristics has been studied experimentally, and some of them were explained by numerical simulation. Continuous-wave laser beam injection to a gain-switched SM VCSEL near the resonance wavelength corresponding to the main polarization mode lasing reduced the pulse timing jitter, narrowed the linewidth, enhanced the pulse amplitude, and shortened the pulse width. An external laser pulse injection of pulse width shorter than the cavity photon lifetime into the SM VCSEL in an orthogonal polarization direction to its main polarization-mode caused a temporal delay of the polarization recovery after PS due to the photon build-up time, and its delay was the minimum at an optimized bias current, which was about 1.5 time above the threshold current. These polarization dynamics were explained by numerical simulation based on the SFM. Polarization-mode bistability existed even in an SM VCSEL of standard circularly cylindrical shape and was used for all-optical flip-flop operation with set and reset injection pulses of order of 3.5~4.5 fJ pulse energy. These low power consumed high-speed all-optical logic operation can be extended to two-dimensional VCSEL arrays, which may be useful for potential high-capacity all-optical signal processing.

Acknowledgments

This work was supported by the Basic Science Research Programs through the National Research Foundation of Korea (NRF) funded by the Korean Ministry of Education, Science and Technology under Grant no. 2009-0084514. The authors gratefully thank Drs. Byeung-Soo Yoo and Jay Roh of Raycan Co., Ltd. for providing with the VCSELs.

References

[1] E. Kapon and A. Sirbu, "Long-wavelength VCSELs: power-efficient answer," *Nature Photonics*, vol. 3, no. 1, pp. 27–29, 2009.

[2] J. M. Noriega, A. Valle, and L. Pesquera, "Timing jitter reduction in gain-switched VCSELs induced by external optical injection," *Optical and Quantum Electronics*, vol. 40, no. 2–4, pp. 119–129, 2008.

[3] S. H. Lee, K. H. Kim, V. M. Deshmukh, D. W. Kim, and M. H. Lee, "Injection laser wavelength-dependent timing jitter reduction of gain-switched single-mode VCSELs," *IEEE Journal of Quantum Electronics*, vol. 46, no. 9, pp. 1327–1331, 2010.

[4] K. H. Jeong, K. H. Kim, S. H. Lee, M. H. Lee, B. S. Yoo, and K. A. Shore, "Optical injection-induced polarization switching dynamics in 1.5-μm wavelength single-mode vertical-cavity surface-emitting lasers," *IEEE Photonics Technology Letters*, vol. 20, no. 10, pp. 779–781, 2008.

[5] A. Hurtado, A. Quirce, A. Valle, L. Pesquera, and M. J. Adams, "Power and wavelength polarization bistability with very wide hysteresis cycles in a 1550 nm VCSEL subject to orthogonal optical injection," *Optics Express*, vol. 17, no. 26, pp. 23637–23642, 2009.

[6] A. Quirce, A. Valle, and L. Pesquera, "Very wide hysteresis cycles in 1550-nm VCSELs subject to orthogonal optical injection," *IEEE Photonics Technology Letters*, vol. 21, no. 17, pp. 1193–1195, 2009.

[7] V. M. Deshmukh, S. H. Lee, D. W. Kim, K. H. Kim, and M. H. Lee, "Experimental and numerical analysis on temporal dynamics of polarization switching in an injection-locked 1.55-μm wavelength VCSEL," *Optics Express*, vol. 19, no. 18, pp. 16934–16949, 2011.

[8] N. C. Gerhardt, M. Y. Li, H. Jähme, H. H. Höpfner, T. Ackemann, and M. R. Hofmann, "Ultrafast spin-induced polarization oscillations with tunable lifetime in vertical-cavity surface-emitting lasers," *Applied Physics Letters*, vol. 99, no. 15, Article ID 151107, 3 pages, 2011.

[9] N. C. Gerhardt and M. R. Hofmann, "Spin-controlled vertical-cavity surface-emitting lasers," *Advances in Optical Technologies*, vol. 2012, Article ID 268949, 15 pages, 2012.

[10] T. Mori, Y. Yamayoshi, and H. Kawaguchi, "Low-switching-energy and high-repetition-frequency all-optical flip-flop operations of a polarization bistable vertical-cavity surface-emitting laser," *Applied Physics Letters*, vol. 88, no. 10, Article ID 101102, 3 pages, 2006.

[11] T. Katayama, T. Ooi, and H. Kawaguchi, "Experimental demonstration of multi-bit optical buffer memory using 1.55-μm polarization bistable vertical-cavity surface-emitting lasers," *IEEE Journal of Quantum Electronics*, vol. 45, no. 11, pp. 1495–1504, 2009.

[12] S. H. Lee, H. W. Jung, K. H. Kim, and M. H. Lee, "All-optical flip-flop operation based on polarization bistability of conventional-type 1.55-μm wavelength single-mode VCSELs,"

Journal of the Optical Society of Korea, vol. 14, no. 2, pp. 137–141, 2010.

[13] S. H. Lee, H. W. Jung, K. H. Kim et al., "1-GHz All-Optical flip-flop operation of conventional cylindrical-shaped single-mode VCSELs under low-power optical injection," *IEEE Photonics Technology Letters*, vol. 22, no. 23, pp. 1759–1761, 2010.

[14] B. Zhang, X. Zhao, L. Christen et al., "Adjustable chirp injection-locked 1.55-μm VCSELs for enhanced chromatic dispersion compensation at 10-Gbit/s," in *Proceedings on Optical Fiber Communication Conference*, San Diego, Calif, USA, February 2008, paper OWT7.

[15] P. Boffi, A. Boletti, A. Gatto, and M. Martinelli, "VCSEL to VCSEL injection locking for uncompensated 40-km transmission at 10 Gb/s," in *Proceedings on Optical Fiber Communication Conference*, San Diego, Calif, USA, March 2009, paper JThA32.

[16] T. B. Gibbon, K. Prince, T. T. Pham et al., "VCSEL transmission at 10 Gb/s for 20 km single mode fiber WDM-PON without dispersion compensation or injection locking," *Optical Fiber Technology*, vol. 17, no. 1, pp. 41–45, 2011.

[17] D. S. Seo, D. Y. Kim, and H. F. Liu, "Timing jitter reduction of gain-switched DFB laser by external injection-seeding," *Electronics Letters*, vol. 32, no. 1, pp. 44–45, 1996.

[18] K. T. Vu, A. Malinowski, M. A. F. Roelens, and D. J. Richardson, "Detailed comparison of injection-seeded and self-seeded performance of a 1060-nm gain-switched Fabry-Pérot laser diode," *IEEE Journal of Quantum Electronics*, vol. 44, no. 7, pp. 645–651, 2008.

[19] M. San Miguel, Q. Feng, and J. V. Moloney, "Light-polarization dynamics in surface-emitting semiconductor lasers," *Physical Review A*, vol. 52, no. 2, pp. 1728–1739, 1995.

[20] I. Gatare, M. Sciamanna, J. Buesa, H. Thienpont, and K. Panajotov, "Nonlinear dynamics accompanying polarization switching in vertical-cavity surface-emitting lasers with orthogonal optical injection," *Applied Physics Letters*, vol. 88, no. 10, Article ID 101106, 2006.

[21] K. H. Jeong, K. H. Kim, S. H. Lee, M. H. Lee, B. S. Yoo, and K. A. Shore, "Polarization switching in a 1.5 μm wavelength single-mode vertical cavity surface emitting laser under modulated optical beam injection control," in *Proceedings of the Photonics in Switching*, San Francisco, Calif, USA, August 2007, paper TuP1.

[22] J. Martin-Regalado, F. Prati, M. San Miguel, and N. B. Abraham, "Polarization properties of vertical-cavity surface-emitting lasers," *IEEE Journal of Quantum Electronics*, vol. 33, no. 5, pp. 765–783, 1997.

[23] A. E. Siegman, *Lasers*, chapters 25 and 13, University Science Books, 1986.

[24] A. Quirce, J. R. Cuesta, A. Hurtado et al., "Dynamic characteristics of an all-optical inverter based on polarization Switching in long-Wavelength VCSELs," *IEEE Journal of Quantum Electronics*, vol. 48, no. 5, pp. 588–595, 2012.